

Transverse-spin asymmetries in COMPASS Drell-Yan data

Małgorzata Niemiec^{a,*}

^a*University of Warsaw,*

Ludwika Pasteura 5, Warsaw, Poland

E-mail: malgorzata.rozalia.niemiec@cern.ch

Studies of the transverse-spin dependent azimuthal asymmetries in the Drell-Yan process permit to access the spin-dependent structure of the nucleon and especially to test the limited universality of its transverse-momentum dependent parton distributions. In 2015 and 2018 the COMPASS Collaboration at CERN performed measurements of the $\pi^- p \rightarrow \mu^+ \mu^- X$ reaction at 190 GeV/c pion beam and transversely polarised NH₃ target. This study covers the measurement of transverse spin asymmetries in Drell-Yan processes, and in particular, introduces a novel approach, in contrast to the conventional one, where the asymmetries were weighted by powers of a transverse momentum of the dimuon system with respect to the beam. This method facilitates the extraction of the transverse-momentum dependent parton distribution functions and opens an easy access to their certain k_T^2 moments. Results of these analyses will be presented.

42nd International Conference on High Energy Physics (ICHEP2024)

18-24 July 2024

Prague, Czech Republic

*Speaker, on behalf of COMPASS Collaboration

1. Introduction

Understanding the internal structure of the nucleon, particularly its spin structure, is critical for advancing theoretical and experimental investigations in particle physics. The quark content of the nucleon in the collinear approximation or after integration over the intrinsic quark transverse momentum k_T is fully specified at the twist-two level by three parton distribution functions (PDFs) for each quark flavour. Two of these functions have been measured with good accuracy: the unpolarised distribution $f_1(x)$, which describes the number density of quarks with flavour q carrying a fraction x of the longitudinal momentum of the fast moving parent nucleon, and the helicity distribution $g_1(x)$, which quantifies the difference between the number densities of quarks with helicity parallel and antiparallel to the spin of the nucleon that is longitudinally polarised. The transversity distribution $h_1(x)$ remains the least understood function of the nucleon structure in the collinear approach owing to its chirally-odd nature. This PDF describes the difference in quark number densities with spins aligned or opposed to the spin of a transversely polarised nucleon. While the collinear approximation provides valuable insights, it simplifies the picture by integrating over the transverse momentum of quarks. To achieve comprehensive three-dimensional description of nucleon structure, it is essential to account for the transverse momentum and spin correlations of partons. In the twist-2 approximation, there are eight transverse-momentum dependent (TMD) PDFs that describe the distributions of longitudinal and transverse momenta of partons and their correlations with the spins of nucleons and quarks. TMD PDFs are accessed via measurements of specific azimuthal asymmetries in reactions like semi-inclusive measurements of hadron production in deep-inelastic lepton-nucleon collisions (SIDIS, $\ell N \rightarrow \ell' h X$) and the Drell-Yan process, where a quark and antiquark annihilate, producing oppositely charged lepton pairs in hadron-nucleon collisions (DY, $h N \rightarrow \ell \ell' X$). In both cases, their cross section can be factorized into convolutions of two components: hard-scattering parton cross sections, calculable using perturbative methods, and non-perturbative functions including PDFs and fragmentation functions. The COMPASS experiment at CERN provides a unique platform for investigating the transverse spin structure of the nucleon through both SIDIS and DY processes.

2. Transverse-Spin Asymmetries in the Drell–Yan Process

The Drell–Yan process occurs through the annihilation of a quark-antiquark pair into a virtual photon, which then produces a pair of oppositely charged leptons. The general expression for the differential cross section at leading twist and leading order for a transversely polarised target is given by [1]:

$$\begin{aligned} \frac{d\sigma_{\text{DY}}}{d^4q d\cos\theta d\varphi_S} = \frac{\alpha^2}{Cq^2} & \left\{ (1 + \cos^2\theta) F_U^1 + \sin^2\theta \cos 2\varphi_{\text{CS}} F_U^{\cos 2\varphi_{\text{CS}}} \right. \\ & + |\mathcal{S}_T| \left[(1 + \cos^2\theta) \sin\varphi_S F_T^{\sin\varphi_S} \right. \\ & + \sin^2\theta \sin(2\varphi_{\text{CS}} + \varphi_S) F_T^{\sin(2\varphi_{\text{CS}} + \varphi_S)} \\ & \left. \left. + \sin^2\theta \sin(2\varphi_{\text{CS}} - \varphi_S) F_T^{\sin(2\varphi_{\text{CS}} - \varphi_S)} \right] \right\}, \end{aligned} \quad (1)$$

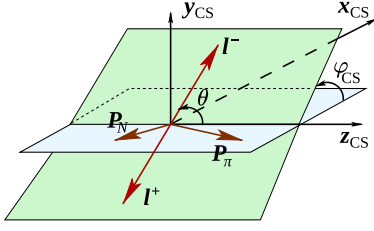


Figure 1: Angles φ_{CS} and θ in the Collins–Soper frame.

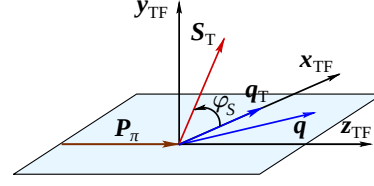


Figure 2: The angle φ_S in the target frame.

where q is a virtual photon momentum, θ is a polar angle of the muon momentum l^- in the Collins–Soper frame shown in Fig. 1, and a kinematic factor $C = 4\sqrt{(P_\pi \cdot P_N)^2 - M_\pi^2 M_p^2}$, with P_π, P_N representing the four-momenta of the pion and nucleon. Meanwhile, φ_{CS} refers to the azimuthal angle of l^- in the Collins–Soper frame, while φ_S denotes the azimuthal angle of the target polarization vector S_T in the target frame (Fig. 2). Each term includes a structure function $F_{U/T}^X$, which is expressed as a flavour-weighted sum of convolutions of TMD PDFs over the intrinsic momenta of the two annihilating quarks, one from the pion ($\mathbf{k}_{T,\pi}$) and the other from the proton ($\mathbf{k}_{T,p}$). The subscript of the structure function indicates the polarization state of the target nucleon, with ‘U’ for contributions independent of polarization and ‘T’ for those from transverse polarization. The superscript denotes the azimuthal modulation.

Spin effects are relatively small, making it more efficient to measure the transverse spin dependent azimuthal asymmetries (TSAs) rather than the structure functions directly. The TSAs correspond to the amplitudes of the azimuthal modulations of the cross section in terms of the structure functions, and can be expressed as follows:

$$A_T^{\sin \varphi_S} = \frac{F_T^{\sin \varphi_S}}{F_U^1}, \quad A_T^{\sin(2\varphi_{CS} \pm \varphi_S)} = \frac{F_T^{\sin(2\varphi_{CS} \pm \varphi_S)}}{2F_U^1}. \quad (2)$$

3. Principle of the Transverse-Momentum Weighting

The convolution over \mathbf{k}_T in the structure function F_U^1 , which appears in the denominator of Eq. 2, simplifies to a flavour sum of products of collinear (i.e. \mathbf{k}_T -integrated) PDFs after integrating over transverse component of virtual photon momentum $\mathbf{q}_T = \mathbf{k}_{T,\pi} + \mathbf{k}_{T,p}$. In contrast, resolving the convolution in the structure function $F_T^{\sin \varphi_S}$ in the numerator of Eq.2, requires the assumption of a specific \mathbf{k}_T -dependence for the TMD PDFs. An alternative approach involves weighting the spin-dependent part of the cross-section by appropriate powers of the outgoing particle transverse momentum. This method was first introduced in the context of SIDIS [2], but the formalism has been later applied to DY processes as well. The weighted asymmetries exploit the fact that, by integrating the structure functions over \mathbf{q}_T with appropriately chosen weight, the convolutions simplify significantly, similar to the case of F_U^1 .

The q_T -weighted transverse-spin asymmetries (WTSAs) can then be expressed as simple products of TMD PDFs for the pion (π^-) and proton (p), or as certain moments of these distributions,

defined as:

$$f_h^{(n)}(x) = \int d^2\mathbf{k}_T \left(\frac{k_T^2}{2M_h^2} \right)^n f(x, k_T^2), \quad (3)$$

where M_h is the mass of the hadron.

The Siverts, pretzelosity, and transversity asymmetries discussed in this paper are subsequently expressed as follows:

$$\begin{aligned} A_T^{\sin\varphi_S \frac{q_T}{M_p}} &= \frac{\int d^2\mathbf{q}_T \frac{q_T}{M_p} F_T^{\sin\varphi_S}}{\int d^2\mathbf{q}_T F_U^1} = -2 \frac{\sum_q e_q^2 [f_{1,\pi^-}^{\bar{q}}(x_\pi) f_{1T,p}^{\perp(1)q}(x_N) + (q \leftrightarrow \bar{q})]}{\sum_q e_q^2 [f_{1,\pi^-}^{\bar{q}}(x_\pi) f_{1,p}^q(x_N) + (q \leftrightarrow \bar{q})]}, \\ A_T^{\sin(2\varphi_{CS}+\varphi_S) \frac{q_T^3}{2M_\pi M_p^2}} &= \frac{\int d^2\mathbf{q}_T \frac{q_T^3}{2M_\pi M_p^2} F_T^{\sin(2\varphi_{CS}+\varphi_S)}}{\int d^2\mathbf{q}_T F_U^1} = -6 \frac{\sum_q e_q^2 [h_{1,\pi^-}^{\perp(1)\bar{q}}(x_\pi) h_{1T,p}^{\perp(2)q}(x_N) + (q \leftrightarrow \bar{q})]}{\sum_q e_q^2 [f_{1,\pi^-}^{\bar{q}}(x_\pi) f_{1,p}^q(x_N) + (q \leftrightarrow \bar{q})]}, \\ A_T^{\sin(2\varphi_{CS}-\varphi_S) \frac{q_T}{M_\pi}} &= \frac{\int d^2\mathbf{q}_T \frac{q_T}{M_\pi} F_T^{\sin(2\varphi_{CS}-\varphi_S)}}{\int d^2\mathbf{q}_T F_U^1} = -2 \frac{\sum_q e_q^2 [h_{1,\pi^-}^{\perp(1)\bar{q}}(x_\pi) h_{1,p}^q(x_N) + (q \leftrightarrow \bar{q})]}{\sum_q e_q^2 [f_{1,\pi^-}^{\bar{q}}(x_\pi) f_{1,p}^q(x_N) + (q \leftrightarrow \bar{q})]}. \end{aligned} \quad (4)$$

In this expression, f_1, h_1 represent the unpolarised quark number density and the transversity distribution, while $f_{1T,p}^{\perp(1)}$, $h_1^{\perp(1)}$, $h_{1T}^{\perp(2)}$ are not TMD PDFs themselves but correspond to the first moments of the Siverts and Boer-Mulders, and the second moment of pretzelosity distribution.

4. Results

The COMPASS DY data collected in 2015 and 2018 utilized a π^- meson beam with a momentum of 190 GeV/c, provided by the CERN SPS. The beam was scattered off a solid-state NH₃ target, with approximately 73% of the hydrogen nuclei transversely polarised. The target comprised two cylindrical cells aligned longitudinally, with vertical polarization in opposite directions, enabling the simultaneous collection of data for both spin orientations. A comprehensive description of the COMPASS spectrometer can be found in Ref. [3]. The standard TSAs were measured within the dimuon mass range $4.0 < M_{\mu\mu}$ (GeV/c²) < 9.0 [4], while the WTSAs were evaluated for the range $4.3 < M_{\mu\mu}$ (GeV/c²) < 8.5 . The TSAs were calculated in one-dimensional kinematic bins of x_N , x_π , the dimuon Feynman variable x_F , q_T , and $M_{\mu\mu}$. The combined results for the three TSAs are presented in Fig. 3. Meanwhile, the WTSAs are presented in Fig. 4 as functions of x_N , x_π , x_F , $M_{\mu\mu}$, and integrated over all mentioned variables.

The Siverts asymmetry is predicted to be positive across the entire kinematic range, a trend that is consistently reflected in the COMPASS data, as illustrated in Fig. 3. In Fig. 5 the Siverts TSA is presented alongside model predictions, evaluated both with and without the sign-change hypothesis. These are represented by dark-shaded curves in the upper section and light-shaded curves in the lower section of the figure, respectively. The range of model predictions indicates that the COMPASS measurement aligns with the sign-change hypothesis within one standard deviation, while diverging from the no-sign-change hypothesis by about three standard deviations. This finding is also consistent with the Siverts WTSAs results, which lie one standard deviation above zero.

Transversity asymmetries are anticipated to be negative, but the magnitude of this effect is

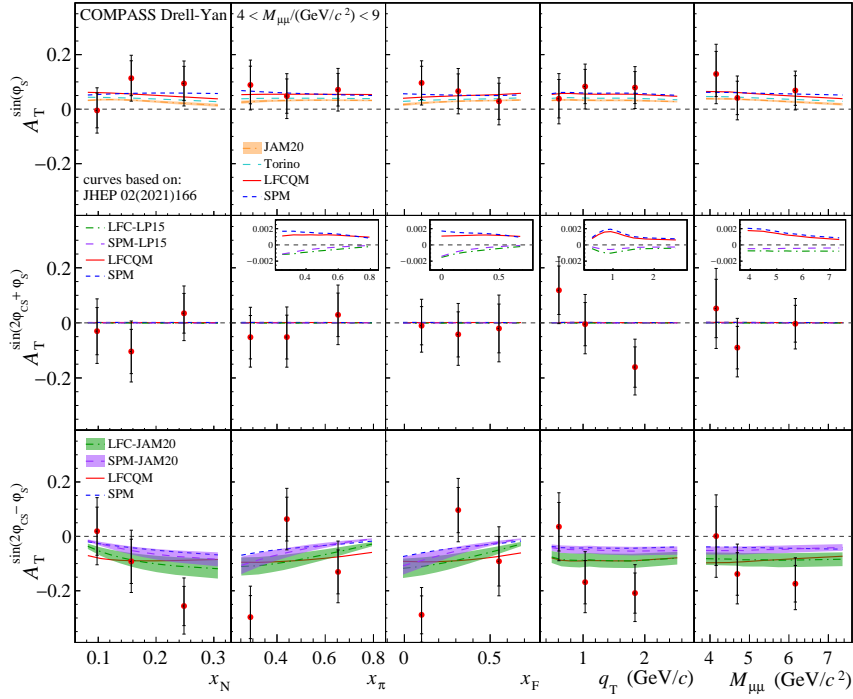


Figure 3: Kinematic dependences of the Siverson, pretzelosity, and transversity TSA (top to bottom) [4] with theoretical curves [5]. Inner (outer) error bars represent statistical (total experimental) uncertainties.

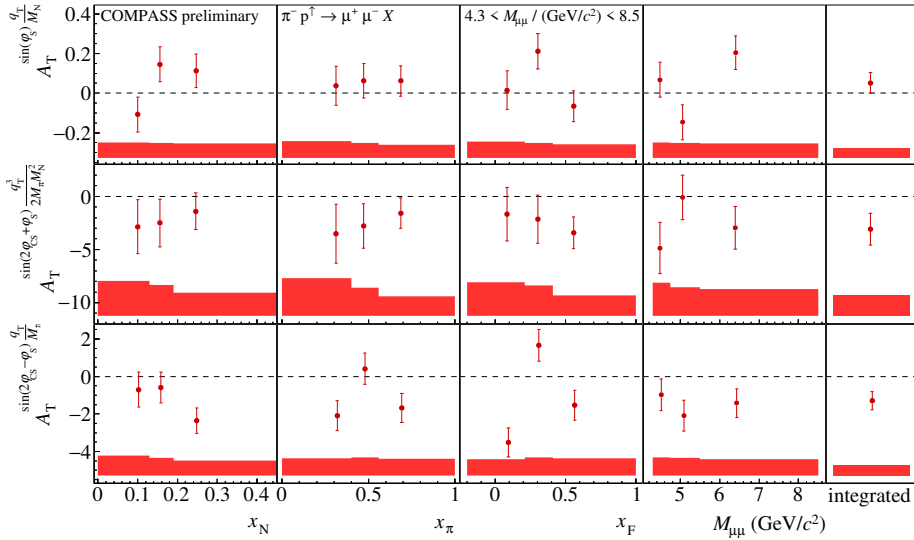


Figure 4: Kinematic dependences of the Siverson, pretzelosity, and transversity WTSA (top to bottom). Error bars (error bands) represent statistical (systematic) uncertainties.

larger in absolute value compared to the Siverson TSA [5]. The measured average value for the transversity TSA, shown in Fig. 6 is indeed negative, with a significance of approximately two

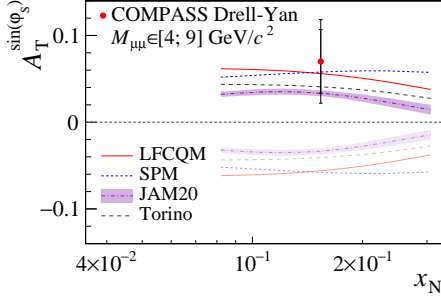


Figure 5: Measured average Sivers TSA and theoretical predictions from different models [4].

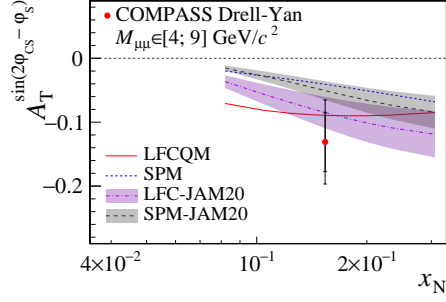


Figure 6: Measured average transversity TSA and theoretical predictions from different models [4].

standard deviations. This supports the universal nature of the transversity TMD PDFs. Similarly, the transversity WTSA also exhibits a negative value, reinforcing this overall trend.

Due to the relatively low magnitude of the pretzelosity TMD PDFs and the effects of kinematic suppression, pretzelosity asymmetries are predicted to be very small [5]. Consistent with these predictions, the average values for TSAs are small and compatible with zero within the uncertainties. For the WTSAs, the measured asymmetries are approximately one standard deviation below zero, influenced by the cubic dependence on q_T , which emphasizes the region of large q_T where the TSA is negative. This cubic weighting drives the asymmetry values negative. In contrast, the effect does not affect the other asymmetries, as their dependence on q_T is linear.

5. Conslusions

The investigation of transverse-spin asymmetries in the Drell-Yan measured by the COMPASS Collaboration provides unique new inputs for the study of the nucleon TMD PDFs and their universality properties. The TSA analysis is consistent with theoretical predictions. Through the novel approach of transverse-momentum weighting, TMD PDFs can be extracted without struggling with convolution over transverse momenta. The results for the Sivers and transversity WTSAs align well with theoretical expectations. The pretzelosity WTSA values exhibit a negative shift due to the weighting method employed.

References

- [1] S. Arnold, A. Metz and M. Schlegel, Phys. Rev. D **79**,034005 (2009), arXiv: arXiv:0809.2262.
- [2] A. M. Kotzinian, P. J. Mulders, Phys. Rev. D **54**, 1229 (1996), arXiv:hep-ph/9511420.
- [3] P. Abbon *et al.*, COMPASS Collaboration, Nucl. Instrum. Meth. A **577**, 455 (2007), arXiv:hep-ex/0703049.
- [4] COMPASS Collaboration, Phys. Rev. Lett. **133**, 071902 (2024), arXiv:2312.17379.
- [5] S. Bastami *et al.*, JHEP **02**, 166 (2021), arXiv:2005.14322.